


Thermal performance of liquid metal phase heat exchanger used in hydrogen production by thermal efficiency method

 <https://doi.org/10.56238/sevned2024.004-022>

Élcio Nogueira¹ and Diniz Felix dos Santos Filho²

ABSTRACT

The main objective of the work is to apply the thermal efficiency method to analyze the heat exchange process in a heat exchanger used in a nuclear power plant to produce hydrogen. The fluids that exchange heat are superheated Helium and the liquid metal Sodium, the first used as the primary refrigerant and the second as the secondary heat exchanger refrigerant. The presented solution is restricted to the heat exchange and considers the two-phase heat exchange process as a nucleated boiling heat exchange for Sodium. The quantities determined for global heat transfer process analysis are thermal efficiencies, thermal effectiveness, heat transfer rates, and fluid exit temperatures in the three heat exchange regions by the liquid metal Sodium: subcooled fluid, saturated steam, and superheated steam. The theoretical analysis is a powerful tool that makes it possible to analyze situations under different operating conditions, which are not permissible through experimental means due to the high cost involved. The results are compared with the literature, and the absolute deviation for the quantities under analysis does not exceed 13%. The use of the equation developed by Rhosenow in 1963 for nucleated boiling heat exchange proved consistent in the simulation presented.

Keywords: Liquid metal, Heat exchanger, Produce of hydrogen, Nuclear power plant, Thermal efficiency.

¹ Doctor

Academic Institution: AEDB/UniDomBosco, UNIFOA, UERJ (Retired!)

E-mail: elcionogueira@hotmail.com

² Master

Academic Institution: AEDB/UniDomBosco, UNIFOA, UERJ

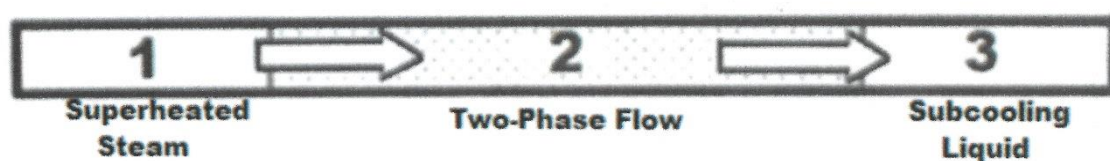
INTRODUCTION

The main objective of the work is to apply the thermal efficiency method to analyze the heat exchange process in a heat exchanger used in a nuclear power plant to generate electricity and produce hydrogen. During hydrogen production, it becomes necessary to use a heat exchanger to transfer heat from the Nuclear Power Plant (NPP) to the hydrogen plant efficiently. For this purpose, phase change heat exchangers are the most suitable due to the high enthalpy transfer. This energy transfer includes the heat associated with the superheated vapor, the latent heat of vaporization, and the liquid's sensible heat. The fluids that exchange heat are Helium and Sodium, the first used as the primary refrigerant and the second as the secondary heat exchanger refrigerant.

Sodium is a liquid metal that behaves like a Newtonian fluid. It is desirable for transferring energy to process plants as a secondary medium since it has high thermal conductivity and allows high heat transfer coefficients. Another advantage of Sodium is that it can act close to atmospheric pressure due to its high standard boiling point. The saturation temperature of Sodium in the two-phase heat exchange region equals 833 °C.

In this work, Helium superheated by the nuclear reactor enters the heat exchanger at 1027 °C. Sodium enters the heat exchanger from the opposite end at 120 °C as a subcooled liquid. The Liquid Metal Phase Heat Exchanger - LMPHE under analysis is a counterflow heat exchanger with three distinct sections: the superheated helium vapor inlet Region 1, Region 2, where the sodium convective boiling process occurs, and the subcooled liquid of sodium inlet Region 3, as schematically shown in Figure 1. Arrows indicate the direction of the helium flow.

Figure 1 – Liquid Metal Phase Heat Exchanger Process



The theoretical analysis is a powerful tool, making it possible to analyze situations under different operating conditions, which are not permissible through experimental means due to the high cost involved. The analytical solution is restricted to the heat exchange aspect and considers the two-phase heat exchange process as a nucleated boiling heat exchange for Sodium. The quantities determined for global heat transfer process analysis are thermal efficiencies, thermal effectiveness, heat transfer rates, and fluid exit temperatures in the three regions described above.

Piyush Sabharwall et al.^[1] developed a design for a heat exchanger coupled to a nuclear reactor and associated with a hydrogen production plant. The reactor supplies energy in heat to the primary helium coolant, heated to outlet temperatures of 1100 to 1300 K and flowing through a high-

temperature heat exchanger, where heat exchange with Sodium occurs. The heat exchanger studied is a way to efficiently transfer thermal energy from the Nuclear Power Plant to the hydrogen production facility. The authors perform a detailed analytical solution for the phase change heat exchanger and determine the global heat transfer coefficients and pressure drop for the three phases associated with Sodium: subcooled liquid, saturated steam, and superheated steam. Sodium is the most promising for heat transport among alkali metals because it has high thermal conductivity and heat transfer coefficients and behaves like Newtonian fluids. They clarify that the difference between liquid metals and non-metallic fluids is that the former have high boiling points, can operate close to atmospheric pressure, and are more sensitive to boundary conditions. They determine that the global heat exchange coefficient in the saturated vapor section equals $228.38 \text{ W}/(\text{m}^2 \text{ K})$ when operating at a speed equal to half the sonic velocity and in the subcooled liquid area, similar to $338.19 \text{ W}/(\text{m}^2 \text{ K})$. When the operating speed in the saturated vapor region equals $1/4$ of the sonic velocity, the heat transfer coefficient equals $272.27 \text{ W}/(\text{m}^2 \text{ K})$. They use the well-known Chen correlation to calculate the global heat transfer coefficient in the saturated vapor region, which considers micro and macro heat exchange mechanisms. However, they conclude that the overall heat transfer coefficient is more influenced by helium vapor. They believe the study could be helpful in experimental work related to phase change heat exchangers.

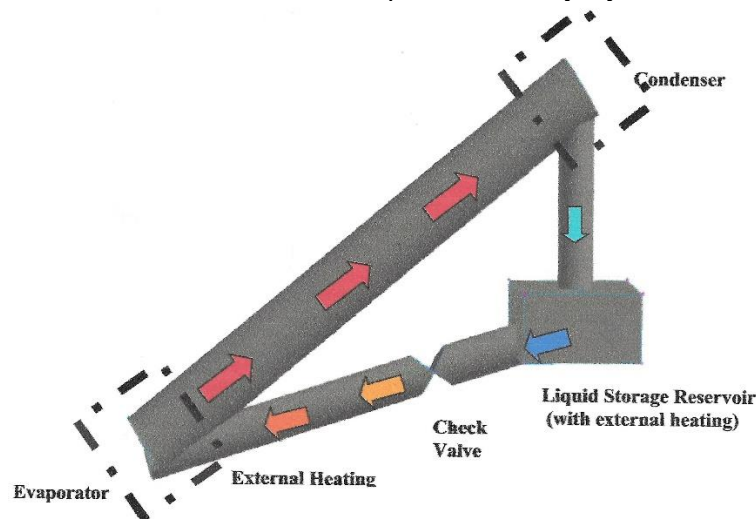
Idaho National Laboratory (United States)^[2] presents a report on designing, constructing, and operating a prototype nuclear reactor to produce hydrogen. The prototype aims to provide an economically competitive nuclear heat source with minimal risk and regular hydrogen production capacity. The reactor outlet temperature is between 800 and 950°C . The development of hydrogen production facilities is of comparable complexity to that of the nuclear reactor, and, in this sense, it is necessary to isolate the two systems using an alternative high-temperature heat source before coupling them. The heat from the high-temperature helium coolant will be used to produce hydrogen. The heat from the high-temperature helium refrigerant will produce hydrogen from heat exchange with liquid metal sodium.

Piyush Sabharwall^[3] argues that a viable option for long-distance thermal energy transport is a single-phase forced convection device mechanically pumping fluid between heat exchangers. This option presents excellent challenges due to the high temperatures involved but can be carried out using a high-temperature thermosiphon, which uses phase change for high temperatures. In this sense, he presents a feasible study for implementing a system that allows thermal energy transfer to a hydrogen production facility relatively far from a nuclear reactor. However, he argues, thermosiphons have operational limitations as they depend on gravitational or centrifugal force to drive the subcooled liquid to the evaporator. Furthermore, the gravitational force is only one of the requirements, as thermosiphon performance depends on the properties of the working fluid,

geometry, temperature, or saturation pressure. In this sense, the two-phase thermosiphon is an ideal candidate where the temperature difference between the fluids is relatively small, as the heat transfer rate per unit of temperature difference, i.e., the heat transfer coefficient, is very high.

Piyush Sabharwall et al.^[4] present a preliminary analysis of the thermal performance of a two-phase thermosiphon (Figure 2) for various types of alkali metals. In the thermosiphon, the working fluid is recirculated with the help of gravitational force, which allows heat transfer to be transported over appreciable distances without the need for external pumping. They clarify that the analysis aims to select high-efficiency compact heat exchangers that work at high temperatures. Furthermore, they present an analysis of a spiral plate heat exchanger and state that this type of heat exchanger is less susceptible to fouling and has never been considered in processes that occur phase change. They believe that the research developed will provide valuable elements for decision-making related to the heat transfer system between the nuclear reactor and the hydrogen production plant.

Figure 2 – Schematic Two-Phase Thermosiphon idealized by Piyush Sabharwall et al.^[4]



Shanbin Shi et al.^[5] argue that heat pipes and thermosiphons are widely used in engineering applications due to the almost isothermal phase change heat transfer mechanism and because they are passive devices. They clarify that modeling the complex phenomena that occur internally to the device is essential for project execution and security analysis. They present a two-phase, one-dimensional flow model developed to study heat pipes that work in steady and transient regimes. Apply specific constitutive equations related to interfacial heat, mass transfer, and film thickness to annular flow for wickless thermosiphons. They recommend future research and new experiments to validate the model developed for high-temperature heat pipes.

Élcio Nogueira^[6] presents thermal and viscous irreversibility concepts, applying the thermal efficiency method and the second law of thermodynamics. He used the thermodynamic Bejan

number in a typical example of a problem related to heat exchange between two fluids by a dimensionless solution for counterflow and parallel flow. Numerical results for thermal efficiency, thermal effectiveness, thermal irreversibility, and viscous irreversibility were used to discuss the procedure's advantages. He argues that the system has been applied to many associated heat exchanger problem solutions over the last three years.

Nogueira, É.^[7] presents theoretical work with localized application of the thermal efficiency method to save energy in air conditioning systems with heat pipes with individual fins. The performance analysis uses the number of fins per heat pipe, the number of heat pipes, and fluid inlet temperatures as input parameters. Freon 404A is a working fluid for energy absorption in the evaporator and energy recovery in the Condenser. The theoretical results obtained by the theoretical model located in the Evaporator, Condenser, and globally for the heat exchanger regions are compared with experimental results. Air velocities, Nusselt numbers, thermal efficiencies, heat transfer rates, and exit temperatures were obtained for theoretical-experimental comparison. Global comparisons showed excellent agreement, demonstrating that the localized theoretical approach is a consistent analysis tool for applying finned heat pipes to heat exchangers.

Andrijana D. Stojanović et al.^[8] reaffirm the importance of understanding the heat transfer process in nucleated boiling and accurately predicting the conditions that lead to the critical flow situation, mainly for safety reasons in nuclear power plants. They present a comprehensive review of heat transfer in nucleated boiling and discuss the results of studies related to the heat transfer coefficient in boiling processes and the characteristics associated with the phenomenon. They analyze aspects related to bubble exit diameter, bubble exit frequency, nucleation density, and bubble growth period and the impact reflected in the nucleated boiling process.

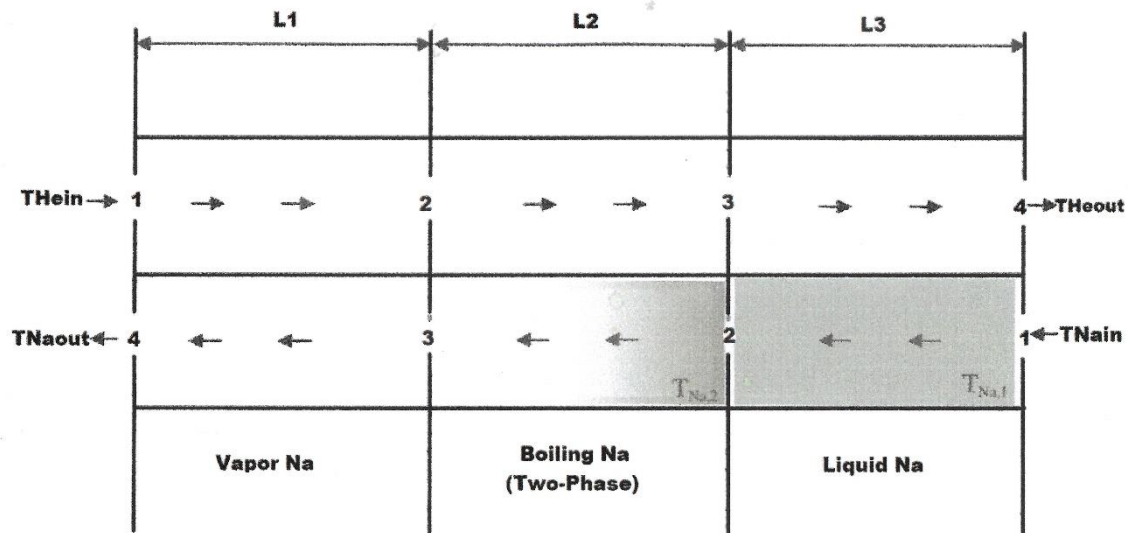
David Taler^[9] proposes new heat transfer correlations in the turbulent flow of liquid metals in tubes with constant heat flow boundary conditions. He used models developed by several researchers in the analysis. He considered the energy conservation equation integrated with the universal profile experimentally determined by Reichart and the different relations for the Prandtl number. He calculated the Nusselt numbers associated with the Reynolds and Prandtl numbers using Lyon Integral. He compared experimental results and adjusted the coefficients to obtain good agreement.

Lei Ren [10] conducted an experimental study on liquid metal as a working fluid. He suggests that large-scale turbulent circulation occurs near the beginning of the convection process. It determines that the evolution in the turbulent flow regime is characterized by the Nusselt number and that the temperature probability density function of the temperature fluctuation in the center of the cell evolves in a Gaussian manner before the turbulent transition to an exponential form in an utterly turbulent regime.

METHODOLOGY

The heat exchange process between the superheated Helium and changing phase sodium is simulated in a heat exchanger composed of three regions, as shown in Figure 3.

Figure 3 – Schematic of Liquid Metal Phase Heat Exchanger (Adapted by Piyush Sabharwall et al.^[1])



The heat exchanger is of the counterflow type, with superheated Helium entering at one end and Sodium as a subcooled liquid in another. The tubes are concentric, and Sodium flows through the inner tube. The saturation temperature of Sodium equals 833 °C and serves as a reference for the three regions. Two different diameters were used for analysis in the saturated vapor region for Sodium. The minor diameter is related to half the speed of sound in the pipe, and the largest diameter is to $\frac{1}{4}$ the speed of sound. It is assumed that the thermal resistance associated with the tube surface is negligible compared to the thermal resistance related to the fluids and flow regime. The properties of the fluids are obtained approximately through the mixing temperatures in the regions under analysis.

The physical quantities that remain constant during the analyses are the fluid inlet temperatures, the internal and external diameters in regions 1 and 3, the sodium saturation temperature, and the flow rates. For safety reasons, the inner diameter in the two-phase flow region depends on the assumed speed, which must be lower than the speed of sound associated with sodium^[4].

$$T_{sat} = 833.0 \text{ } ^\circ\text{C fixed}$$

(1)

The saturation temperature of Sodium, T_{sat} , is equal to 833 °C.

$$T_{He_{in1}} = 1027 \text{ } ^\circ\text{C fixed}$$

(2)

THe_{in1} is the inlet temperature of the helium vapor in the heat exchanger.

$$TNa_{in3} = 120 \text{ }^{\circ}\text{C} \text{ fixed}$$

(3)

TNa_{in3} is the temperature at which Sodium enters the heat exchanger.

$$TNa_2 = T_{sat} \text{ fixed}$$

(4)

The saturation temperature of Sodium in region 2 is equal to 833 °C.

$$\dot{m}_{He} = 81.59 \text{ kg/s}$$

(5)

$$D_{He} = 1.551 \text{ m}$$

(6)

The mass flow rate of Helium is 81.59 kg/s, and the external diameter is 1.551 m.

$$\dot{m}_{Na} = 9.794 \text{ kg/s}$$

(7)

$$D_{Na1} = 0.122 \text{ m}$$

(8)

$$D_{Na3} = 0.122 \text{ m}$$

(9)

The mass flow rate of Sodium equals 9.794 kg/s, and the internal diameter in regions 1 and 3 equals 0.122 m.

The properties associated with Helium depend on the vapor mixing temperature in the region under analysis.

$$\begin{aligned} \rho_{Hei} = & 0.1717547693d0 - 0.0005024738072 * THe_i + 9.528424492d - 7 * THe_i ** 2. d0 \\ & - 1.020764019d - 9 * THe_i ** 3. d0 + 5.538255567d - 13 * THe_i ** 4. d0 \\ & - 1.177254392d - 16 * THe_i ** 5. d0 \quad 1 \leq i \leq 3 \end{aligned}$$

(10)

The density of helium vapor is equal to ρ_{Hei} . The Helium mixing temperature in the region under analysis is represented by THe_i , where the index varies from 1 to 3. Petersen, H. ^[11], Vincent D. Arp, and Robert D. McCarty^[12] provide the properties of Helium.

$$k_{Hei} = 0.148407961d0 + 0.0003254147293d0 * THe_i - 4.305657603d - 8 * THe_i ** 2. d0$$

(11)

$$\mu_{Hei} = (1.929583717d0 + 0.004096498682 * THe_i - 5.313746426d - 7 * THe_i ** 2. d0) * 1. d - 5 \quad (12)$$

k_{Hei} is the thermal conductivity of helium vapor in region i. μ_{Hei} is the dynamic viscosity of helium vapor in region i.

$$Pr_{Hei} = 0.6725624682d0 - 2.199176297d - 5 * THe_i + 2.590560079d - 8 * THe_i ** 2. d0 \\ - 2.328029436d - 11 * THe_i ** 3. d0 \\ + 1.17454495d - 14 * THe_i ** 4. d0 - 2.431817654d - 18 * THe_i ** 5. d0$$

(13)

The Prandtl number of Helium in region i is represented by Pr_{Hei} .

$$\nu_{Hei} = \frac{\mu_{Hei}}{\rho_{Hei}}$$

(14)

ν_{Hei} is the dynamic viscosity associated with helium vapor in region i.

$$\alpha_{Hei} = \frac{\mu_{Hei}}{Pr_{Hei}} \quad (15)$$

$$Cp_{Hei} = \frac{\nu_{Hei}}{\alpha_{Hei}} \quad (16)$$

α_{Hei} is the thermal diffusivity of helium vapor in Region i. The specific heat of helium vapor in region i is represented by Cp_{Hei} .

The properties of Sodium in the two-phase flow region are associated with the properties of saturated liquid, related to the index l, and saturated vapor, related to the index v. The properties of Sodium are provided by Joanne K. Fink and Leonard Leibowitz^[13] and by G. H. Golden and J. V. Tokar^[14].

$$\rho_{Nal} = -0.2382637363d0 * TNa_2 + 951.134744d0$$

(17)

$$\rho_{Nav} = (-1942.324038d0 + 9.805341382d0 * TNa_2 - 0.01643668511d0 * TNa_2 ** 2. d0 \\ + 9.251732712d - 6 * TNa_2 ** 3. d0) * 1. d3$$

(18)

$$k_{Nal} = 91.21074266d0 - 0.04824000559d0 * TNa_2 + 6.873126873d - 7 * TNa_2 ** 2. d0$$

(19)

$$k_{Nav} = -0.00578082968d0 + 6.85950024d - 5 * TNa_2 + 6.578942795d - 8 * TNa_2 ** 2. d0 \\ - 1.208200401d - 10 * TNa_2 ** 3. d0 + 4.632867133d - 14 * TNa_2 ** 4. d0$$

(20)

$$\mu_{Nal} = (7.549325321d0 - 0.02161616967d0 * TNa_2 + 3.465090376d - 5 * TNa_2 ** 2. d0 \\ - 3.030746977d - 8 * TNa_2 ** 3. d0 + 1.361249488d - 11 * TNa_2 ** 4. d0 \\ - 2.453808446d - 15 * TNa_2 ** 5. d0) * 1. d - 4$$

(21)

$$\mu_{Nav} = (933.0641319d0 + 1.555217815 * TNa_2 + 0.0003932320867d0 * TNa_2 ** 2. d0 \\ - 1.716200466d - 7 * TNa_2 ** 3. d0) * 1. d - 8$$

(22)

$$Cp_{Na1} = 2.022230309d0 - 0.005312730163d0 * TNa_2 + 1.501227267d - 5 * TNa_2 ** 2. d0 \\ - 2.13879551d - 8 * TNa_2 ** 3. d0 + 1.514270833d - 11 * TNa_2 ** 4. d0 \\ - 4.166666667d - 15 * TNa_2 ** 5. d0$$

(23)

$$Cp_{Nav} = (0.1013238839d0 + 0.002248844802d0 * TNa_2 + 2.089437138d - 5 * TNa_2 ** 2. d0 \\ - 4.723338971d - 8 * TNa_2 ** 3. d0 + 3.569885839d - 11 * TNa_2 ** 4. d0 \\ - 9.307692308d - 15 * TNa_2 ** 5. d0) * 1. d2$$

(24)

$$v_{Na1} = \frac{\mu_{Na1}}{\rho_{Na1}}$$

(25)

$$v_{Nav} = \frac{\mu_{Nav}}{\rho_{Nav}}$$

(26)

$$Pr_{Na1} = \frac{v_{Na1}}{\alpha_{Na1}}$$

(27)

$$Pr_{Nav} = \frac{v_{Nav}}{\alpha_{Nav}}$$

(28)

The density of Sodium is represented by ρ_{Na} , the thermal conductivity by k_{Na} , the dynamic viscosity by μ_{Na} , the specific heat by Cp_{Na} , the kinematic viscosity by v_{Na} , and the Prandtl number by Pr_{Na} . The thermal diffusivity is given by $\alpha_{Na} = \frac{k_{Na}}{\rho_{Na}Cp_{Na}}$.

The energy per unit of mass exchanged between the fluids during two-phase flow in Region 2 is given by:

$$h_{Na1v} = (4771.697082d0 - 1.000857055d0 * TNa_2 - 0.0001022855894d0 * TNa_2 ** 2. d0 \\ + 9.906759907d - 8 * TNa_2 ** 3. d0) * 1. d3$$

(29)

The properties of Sodium in Regions 1 and 3 are obtained by:

$$\rho_{Na1} = -0.2382637363d0 * TNa_1 + 951.134744d0$$

(30)

$$k_{Na1} = 91.21074266d0 - 0.04824000559d0 * TNa_1 + 6.873126873d - 7 * TNa_1 ** 2. d0$$

(31)

$$\mu_{Na1} = (7.549325321d0 - 0.02161616967d0 * TNa_1 + 3.465090376d - 5 * TNa_1 ** 2. d0 \\ - 3.030746977d - 8 * TNa_1 ** 3. d0 + 1.361249488d - 11 * TNa_1 ** 4. d0 \\ - 2.453808446d - 15 * TNa_1 ** 5. d0) * 1. d - 4$$

□

(32)



$$Cp_{Na1} = 2.022230309d0 - 0.005312730163d0 * TNa_1 + 1.501227267d - 5 * TNa_1 ** 2. d0 \\ - 2.13879551d - 8 * TNa_1 ** 3. d0 + 1.514270833d - 11 * TNa_1 ** 4. d0 \\ - 4.166666667d - 15 * TNa_1 ** 5. d0$$

(33)

$$v_{Na1} = \frac{\mu_{Na1}}{\rho_{Na1}}$$

(34)

$$Pr_{Na1} = \frac{v_{Na1}}{\alpha_{Na1}}$$

(35)

$$\rho_{Na3} = (-1942.324038d0 + 9.805341382d0 * TNa_3 - 0.01643668511d0 * TNa_3 ** 2. d0 \\ + 9.251732712d - 6 * TNa_3 ** 3. d0) * 1. d3$$

(36)

$$k_{Na3} = -0.00578082968d0 + 6.85950024d - 5 * TNa_3 + 6.578942795d - 8 * TNa_3 ** 2. d0 \\ - 1.208200401d - 10 * TNa_3 ** 3. d0 + 4.632867133d - 14 * TNa_3 ** 4. d0$$

(37)

$$\mu_{Na3} = (933.0641319d0 + 1.555217815 * TNa_3 + 0.0003932320867d0 * TNa_3 ** 2. d0 \\ - 1.716200466d - 7 * TNa_3 ** 3. d0) * 1. d - 8$$

(38)

$$Cp_{Na3} = (0.1013238839d0 + 0.002248844802d0 * TNa_3 + 2.089437138d - 5 * TNa_3 ** 2. d0 \\ - 4.723338971d - 8 * TNa_3 ** 3. d0 + 3.569885839d - 11 * TNa_3 ** 4. d0 \\ - 9.307692308d - 15 * TNa_3 ** 5. d0) * 1. d2$$

(39)

$$v_{Na3} = \frac{\mu_{Na3}}{\rho_{Na3}}$$

(40)

$$Pr_{Na3} = \frac{v_{Na3}}{\alpha_{Na3}}$$

(41)

The temperatures TNa_1 and TNa_3 are mixing temperatures in the regions under analysis.

$$A_{Hei} = \frac{\pi(D_{He}^2 - D_{Nai}^2)}{4} \quad 1 \leq i \leq 3$$

(42)

The helium flow area is represented by A_{Hei} .

$$Per_{Hei} = \pi(D_{He} + D_{Nai}) \quad 1 \leq i \leq 3$$

(43)

$$Dh_{Hei} = \frac{4A_{Hei}}{Per_{Hei}} \quad 1 \leq i \leq 3$$

(44)

Dh_{Hei} is the hydraulic diameter associated with Helium.



$$Re_{Hei} = \frac{\dot{m}_{He} D_{h_{Hei}}}{A_{Hei} \mu_{Hei}} \quad 1 \leq i \leq 3$$

(45)

$$V_{Hei} = \frac{\dot{m}_{He}}{\rho_{Hei} A_{Hei}} \quad 1 \leq i \leq 3$$

(46)

The Reynolds number associated with Helium is represented by Re_{Hei} , and the velocity by V_{Hei} .

$$Nu_{Hei} = 0.022 Re_{Hei}^{0.8} Pr_{Hei}^{0.5} \quad 1 \leq i \leq 3$$

(47)

Nu_{Hei} is the Nusselt number associated with helium vapor given by W. M. Kays and M. E. Crawford^[15].

$$h_{Hei} = \frac{Nu_{Hei} k_{Hei}}{D_{h_{Hei}}} \quad 1 \leq i \leq 3$$

(48)

The convection heat transfer coefficient is represented by h_{Hei} .

$$A_{Nai} = \frac{\pi D_{Nai}^2}{4} \quad 1 \leq i \leq 3$$

(49)

The sodium flow area is represented by A_{Nai} .

$$Per_{Nai} = \pi D_{Nai}^2 \quad 1 \leq i \leq 3$$

(50)

$$D_{h_{Nai}} = \frac{4A_{Nai}}{Per_{Nai}} \quad 1 \leq i \leq 3$$

(51)

$D_{h_{Nai}}$ is the hydraulic diameter associated with Sodium.

$$Re_{Nai} = \frac{\dot{m}_{Nai} D_{h_{Nai}}}{A_{Nai} \mu_{Nai}} \quad 1 \leq i \leq 3$$

(52)

$$V_{Nai} = \frac{\dot{m}_{Nai}}{\rho_{Nai} A_{Nai}} \quad 1 \leq i \leq 3$$

(53)

The Reynolds number associated with Sodium is represented by Re_{Nai} , and the velocity by V_{Nai} .

$$Nu_{Nai} = 6.3 + Re_{Nai}^{0.85} Pr_{Nai}^{0.93} \quad i = 1 \text{ or } i = 3$$

(54)

Nu_{Nai} is the Nusselt number associated with Sodium in the single-phase region given by W. M. Kays and M. E. Crawford^[1;15].

$$h_{Nai} = \frac{Nu_{Nai}k_{Nai}}{Dh_{Nai}} \quad i = 1 \text{ or } i = 3$$

(55)

The convection heat transfer coefficient is represented by h_{Nai} .

$$Uo_i = \frac{1}{\frac{1}{h_{Hei}} + \frac{1}{h_{Nai}}} \quad i = 1 \text{ or } i = 3$$

(56)

The global heat transfer coefficient in the single-phase region, disregarding the thermal resistance associated with the separation surface between the fluids, is represented by Uo_i .

$$h_{boil} = \mu_{Nai} h_{Nai} v \left(g \frac{(\rho_{Nai} - \rho_{Nai v})}{\sigma_{Na}} \right)^{0.5} \left(\frac{Cp_{Nai}}{Csf h_{Nai} Pr_{Nai}} \right)^3 \Delta T_{sat}^2 \quad i = 2$$

(57)

In the two-phase flow region, Region 2, the boiling coefficient, h_{boil} , used in the simulation is associated with the nucleated boiling process, determined experimentally by W. M. Rohsenow^[16], which presumably can be applied to processes related to liquid metals, according to Piyush Sabharwall et al.^[1]. The Rohsenow equation is more uncomplicated and contains parameters that do not consider some complex effects, such as those occurring in convective boiling, such as that developed by J. C. Chen^[17] and used by Piyush Sabharwall et al.^[1].

$$\Delta T_{sat} = T_{He2} - T_{Na2}$$

(58)

ΔT_{sat} is called the saturation temperature difference.

$$\sigma_{Na} == -0.1000989011d0 * T_{Na2} + 204.8458973d0$$

(59)

The surface tension associated with Sodium is represented by σ_{Na} and can be found in a numerical table obtained by Joanne K. Fink and Leonard Leibowitz^[13].

$$Csf = 0.006 \quad \text{fixed!}$$

(60)

The parameter Csf is used in the work developed by W. M. Rohsenow^[16].

$$Uo_i = \frac{1}{\frac{1}{h_{Hei}} + \frac{1}{h_{boil}}} \quad i = 2$$

(61)

The above global heat transfer coefficient, Uo_i , is associated with the boiling process occurring in Region 2.

$$A_{Tri} = \pi D_{Nai} L_i \quad 1 \leq i \leq 3$$

(62)

A_{Tri} is the area of heat exchange between fluids.

$$C_{Nai} = \dot{m}_{Na} C_{p_{Nai}} \quad \text{Region 2}$$

(63)

$$C_{Nav} = \dot{m}_{Na} C_{p_{Nav}} \quad \text{Region 2}$$

(64)

$$C_{Nai} = \dot{m}_{Na} C_{p_{Nai}} \quad i = 1 \text{ or } i = 3$$

(65)

$$C_{Hei} = \dot{m}_{He} C_{p_{Hei}} \quad 1 \leq i \leq 3$$

(66)

$$C_i^* = \frac{C_i^{min}}{C_i^{max}} \quad 1 \leq i \leq 3$$

(67)

C_i^* is the relationship between the fluids' minimum and maximum thermal capacities in region i .

$$NTU_i = \frac{U_o A_{tri}}{C_i^{min}} \quad 1 \leq i \leq 3$$

(68)

The number of thermal units in region i is represented by NTU_i .

$$Fa_i = \frac{NTU_i(1-C_i^*)}{2} \quad 1 \leq i \leq 3$$

(69)

Fa_i is the factor called "Fin Analogy Number" presented in the pioneering work of Fakhri A.^[18] and used in papers developed by Nogueira, É.^[6-7]

$$\eta_{Ti} = \frac{Tanh(Fa_i)}{Fa_i} \quad 1 \leq i \leq 3$$

(70)

The thermal efficiency in region i is given by η_{Ti} .

$$\varepsilon_{Ti} = \frac{1}{\frac{1}{\eta_{Ti} NTU_i} + \frac{1+C_i^*}{2}} \quad 1 \leq i \leq 3$$

(71)

ε_{Ti} is the thermal effectiveness in region i .

$$\dot{Q}_i = \varepsilon_{Ti} C_i^{min} (T_{Heini} - T_{Naini}) \quad 1 \leq i \leq 3$$

(72)

The heat transfer rate between the fluids in region i is obtained by \dot{Q}_i .

$$\dot{Q}_i^{Max} = C_i^{min} (T_{Heini} - T_{Naini}) \quad 1 \leq i \leq 3$$

(73)

\dot{Q}_i^{Max} is the maximum heat transfer rate between the fluids in region i .

$$THe_{outi} = THe_{ini} - \frac{\dot{Q}_i}{C_i^{min}} \quad 1 \leq i \leq 3$$

(74)

THe_{outi} is the vapor helium outlet temperature in region i.

$$TNa_{outi} = TNa_{ini} + \frac{\dot{Q}_i}{C_i^{min}} \quad i = 1 \text{ or } i = 3$$

(75)

TNa_{outi} is the sodium outlet temperature.

RESULTS AND DISCUSSION

The results obtained through the simulation are divided into three parts associated with Sodium: superheated vapor region (Region 1), saturated vapor region (Region 2), and subcooled liquid region (Region 3).

The data stipulated at the entrances and exits of the regions are represented numerically in red.

SUPERHEATED STEAM REGION – REGION 1

Figure 4 – Thermal efficiency in the region 1 (Superheated Steam)

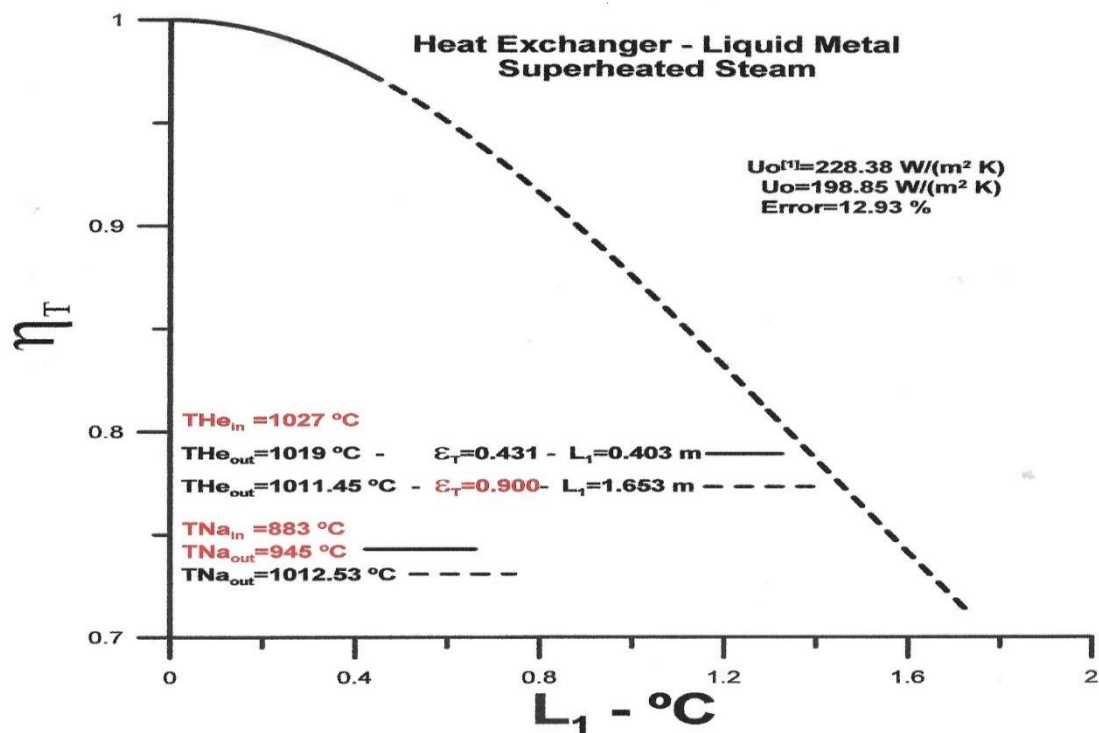


Figure 4 presents values obtained for thermal efficiency in the superheated steam region.

During the simulation, the length of the heat exchange section varies until the exit temperature value stipulated for Sodium is obtained ($T_{Na_{out}}=945\text{ }^{\circ}\text{C}$). In this first imposed situation, the required length of section 1 corresponds to 0.403 meters, and the thermal effectiveness associated with this length is equal to 0.431. In this case, the helium vapor's exit temperature reaches $1019\text{ }^{\circ}\text{C}$. This result is quite conservative since there is a wide margin for improving heat exchange between the fluids, increasing the size of the heat exchange section.

The second situation imposed in the simulation is to increase the thermal efficiency value, improving the heat exchange between the fluids to obtain a higher sodium outlet temperature. In this second simulation, the value imposed for thermal effectiveness is equal to 0.9. The exit temperature of the sodium vapor corresponds to $1012.53\text{ }^{\circ}\text{C}$, and the value for the length of section 1 corresponds to 1.653 m. In this case, the helium vapor's exit temperature reaches $1011.45\text{ }^{\circ}\text{C}$.

There is an effective gain when the demand for heat exchange increases, but in compensation, there is a significant increase in the section length when comparing the first simulation with the second. An essential observation concerning Figure 4 is that the deviation obtained in section 1 for the global heat transfer coefficient equals 12.93%. Note that the section length does not influence the value of the global heat transfer coefficient. The absolute deviation is the result of the simulation concerning the results presented by Piyush Sabharwall et al.^[1].

Figure 5 – Thermal effectiveness in the region 1 (Superheated Steam)

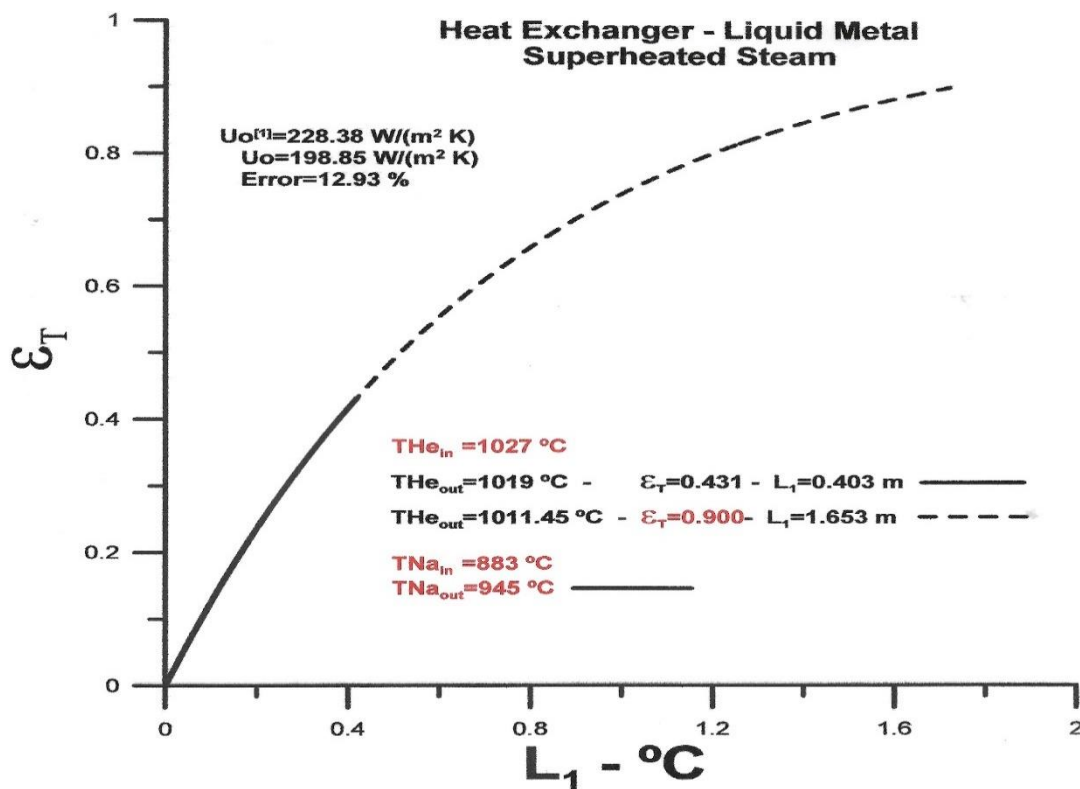


Figure 5 presents values obtained for thermal effectiveness in the superheated steam region.

The results are coherent with the conditions in the simulations related to Figure 4. When the sodium exit temperature is equal to 945 °C, the section length is equal to 0.403 m, and when the effectiveness is equal to 0.9, the section length is equal to 1,657 m.

Figure 6 presents values obtained for heat transfer rate in the superheated steam region.

There is coherence between the results presented for thermal effectiveness and those obtained for the heat transfer rate in Region 1. In the first condition imposed, the heat transfer rate obtained is relatively low when compared to the maximum heat transfer, which depends only on the difference between the inlet temperatures of the helium and sodium fluids. When the effectiveness is set equal to 0.9, the heat transfer rate approaches the maximum, as expected.

Figure 7 presents values obtained for Helium and Sodium outlet temperatures in the superheated steam region.

Again, the exit temperatures for both fluids, Helium and Sodium, are consistent with the conditions imposed in Region 1. When the length of section 1 is equal to 0.403 m, the sodium exit temperature is equal to 945 °C; when the length is equal to 1.653 m, the sodium outlet temperature is equal to 1012.53 °C. The helium temperatures in both conditions equal 1019 °C and 1011.45 °C.

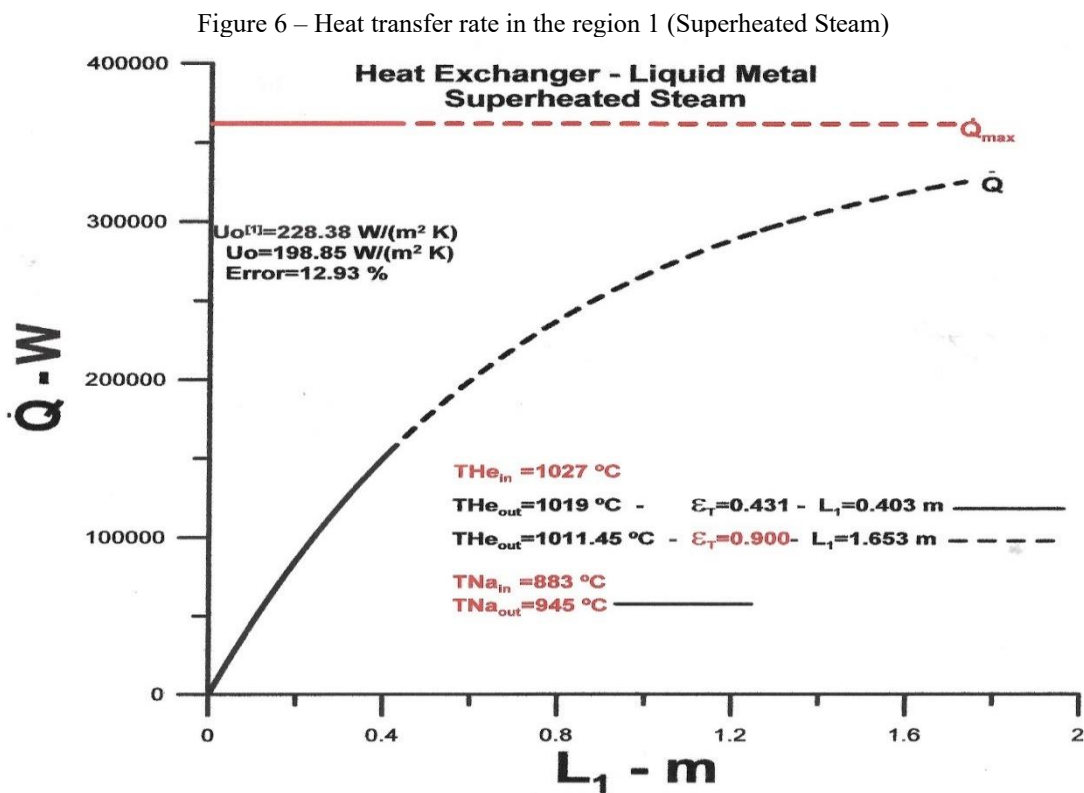
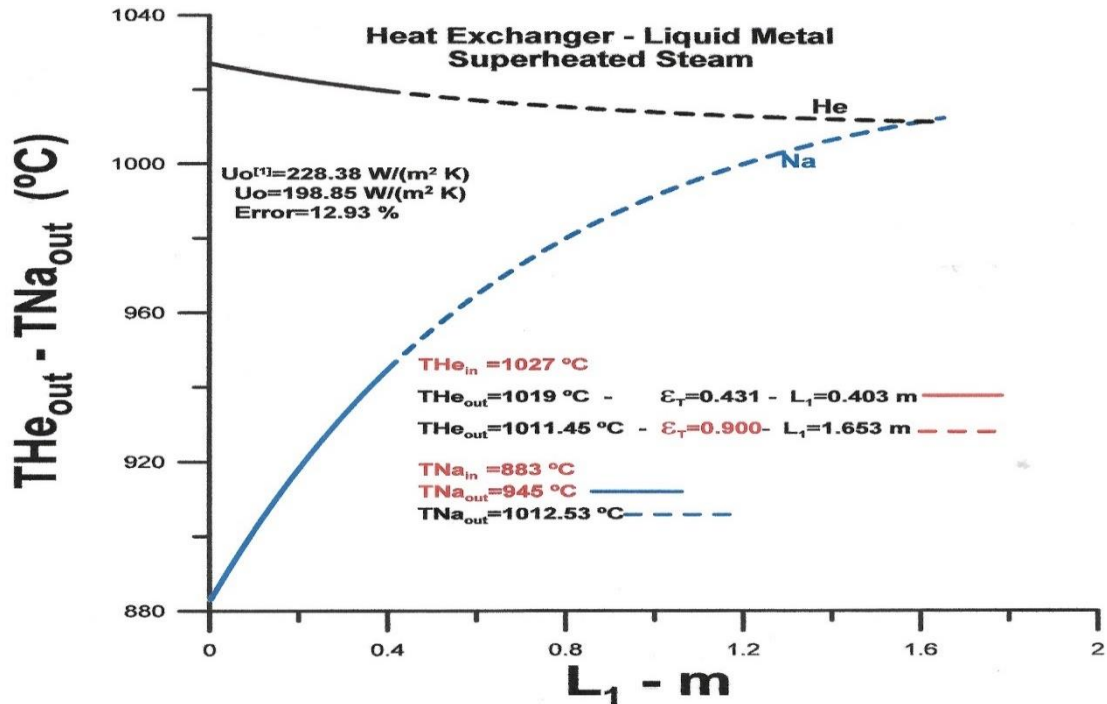


Figure 7 – Outlet temperatures of Helium and Sodium in the region 1 (Superheated Steam)



The helium exit temperatures will influence the results of thermal quantities in Region 2, where Sodium is a saturated vapor.

SATURATED STEAM REGION – REGION 2

In Region 2, saturated vapor for Sodium, the sodium inlet temperature is set equal to 1019 °C, and the sodium temperature is equal to the saturation temperature, equal to 833 °C. However, two new conditions related to the diameter of the tube through which the sodium flows are to be implemented. The speed of sodium vapor cannot exceed the speed of sound, and for safety, the tube diameters must satisfy two conditions: $D_{Na2}=0.1797$ m, which corresponds to half the sonic speed, and $D_{Na2}=0.2542$ m, which corresponds to $\frac{1}{4}$ of the sonic speed.

Figure 8 presents values obtained for thermal efficiency in the saturated steam region.

In addition to the pipe diameter in region 2 being imposed, a second condition must be set to obtain results that allow Sodium to be heated in region 3. The second condition implemented in the simulation relates to the pipe length in Region 2. The size chosen in the implementation must be consistent with the helium exit temperature, and the imposed value equals 0.2 m.

When the imposed diameter corresponds to $\frac{1}{2}$ the speed of sound in the tube, that is, $D_{Na2}=0.1797$ m, the helium exit temperature corresponds to 945 °C, and the exit temperature is 927 °C for a diameter equal to $D_{Na2}=0.2542$ m, which corresponds to $\frac{1}{4}$ the speed of sound. The corresponding values obtained for thermal efficiency are, respectively, 0.544 and 0.678. The higher effectiveness value corresponds to greater heat exchange for the larger diameter. Consistent result with greater heat exchange area.

When comparing the values of the global heat transfer coefficient, there is a deviation of 6.64% related to $\frac{1}{2}$ the speed of sound and 9.05% for $\frac{1}{4}$ the speed of sound. The value used for comparison corresponds to the average value of the global heat transfer coefficient obtained by Piyush Sabharwall et al.[1] in Region 2.

Figure 9 presents values obtained for thermal effectiveness in the saturated steam region.

The thermal effectiveness corresponds to 0.544 in the saturated vapor region when the adopted diameter corresponds to 0.1797 m and 0.678 when the adopted diameter corresponds to 0.2542 m.

Figure 10 presents results for the heat transfer rate in the saturated vapor region, which is compatible with the results shown in Figure 9. In comparison with the maximum heat transfer rate, it is possible to see that the heat exchange is underestimated. However, as there is a need for heating in Region 3, the values obtained are the most realistic possible, considering that the subcooled liquid enters Region 3 at a temperature equal to 120 °C.

Figure 11 shows the temperature profile of Helium in the saturated vapor region associated with Sodium. The outlet temperature corresponds to 945 °C for a diameter of the tube that transposes the Sodium equal to 0.1797 m and is 927 °C for a diameter equal to 0.2542 m. The helium exit temperature values will impact heat transfer in region 1 of subcooled fluid.

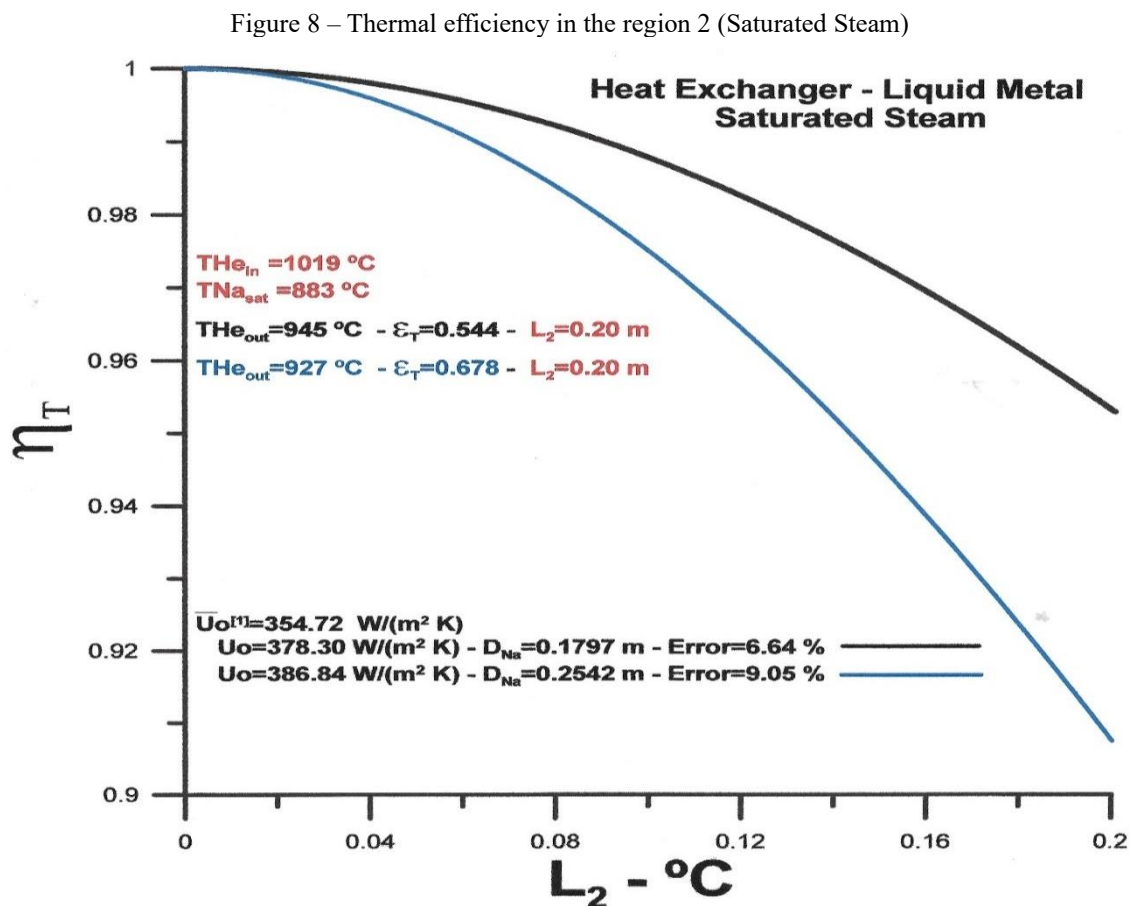


Figure 9 – Thermal effectiveness in the region 2 (Saturated Steam)

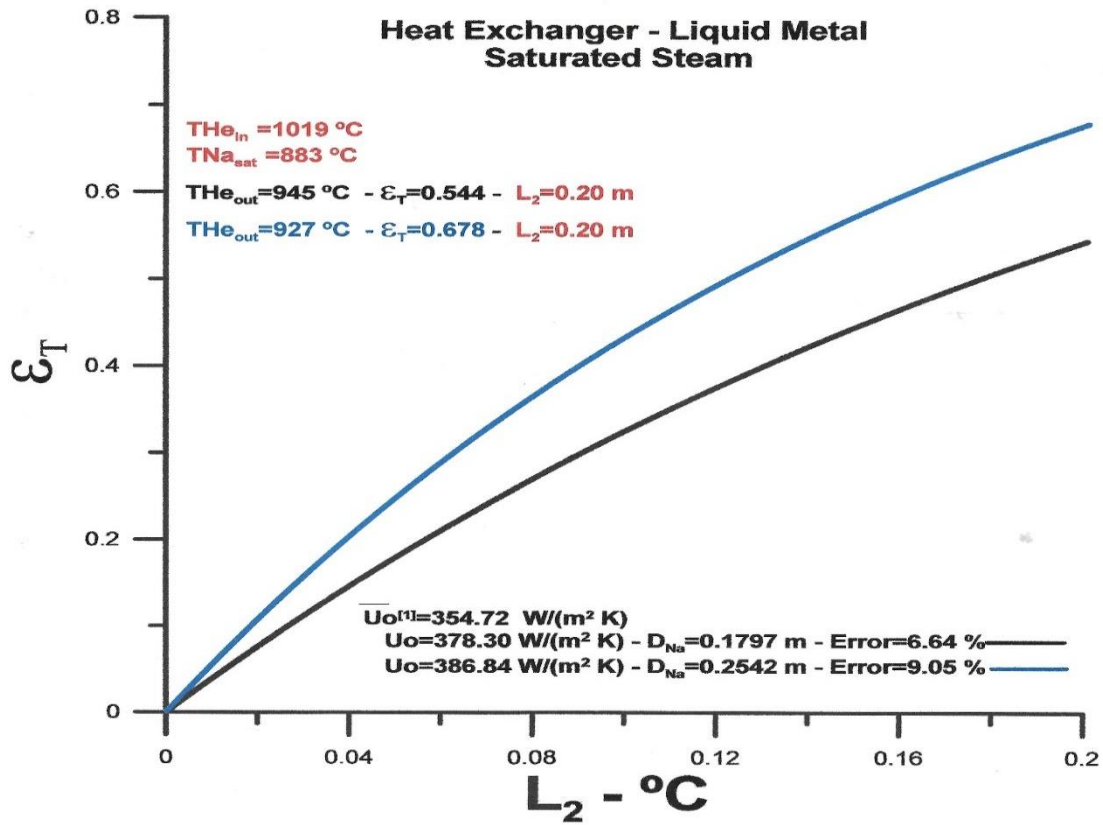


Figure 10 – Heat transfer rate in the region 2 (Saturated Steam)

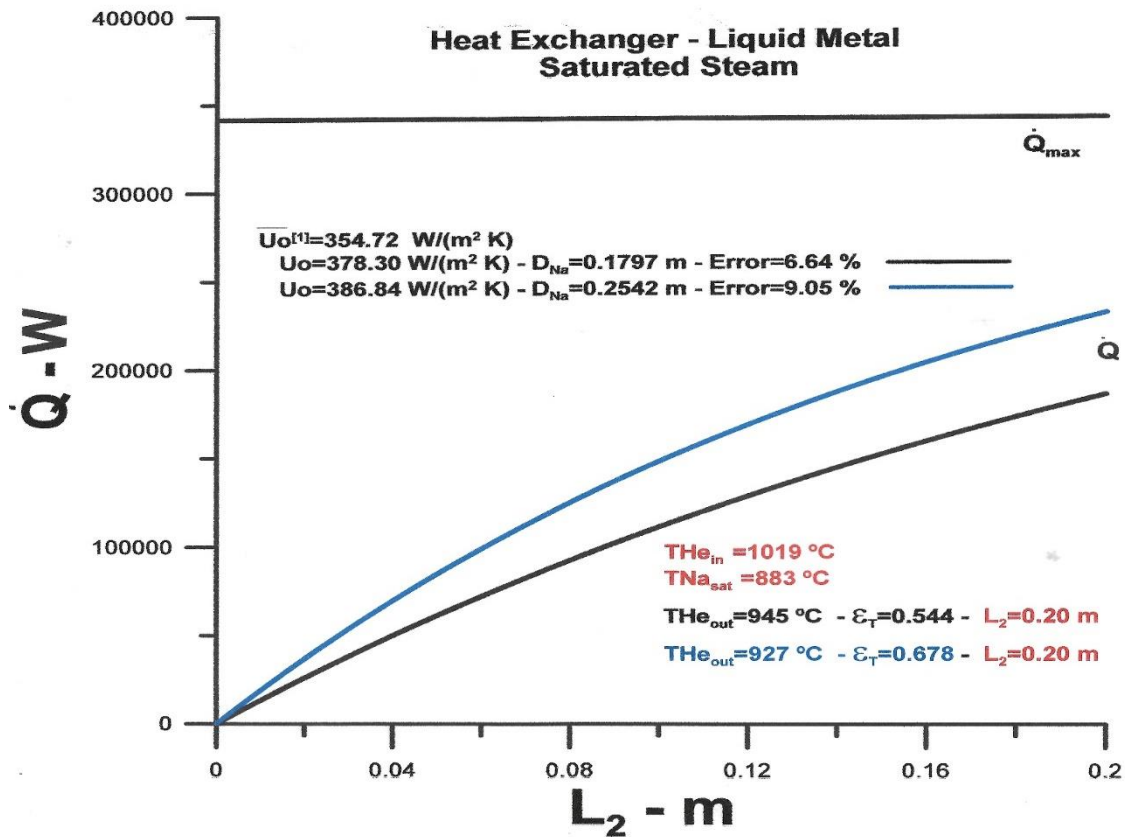
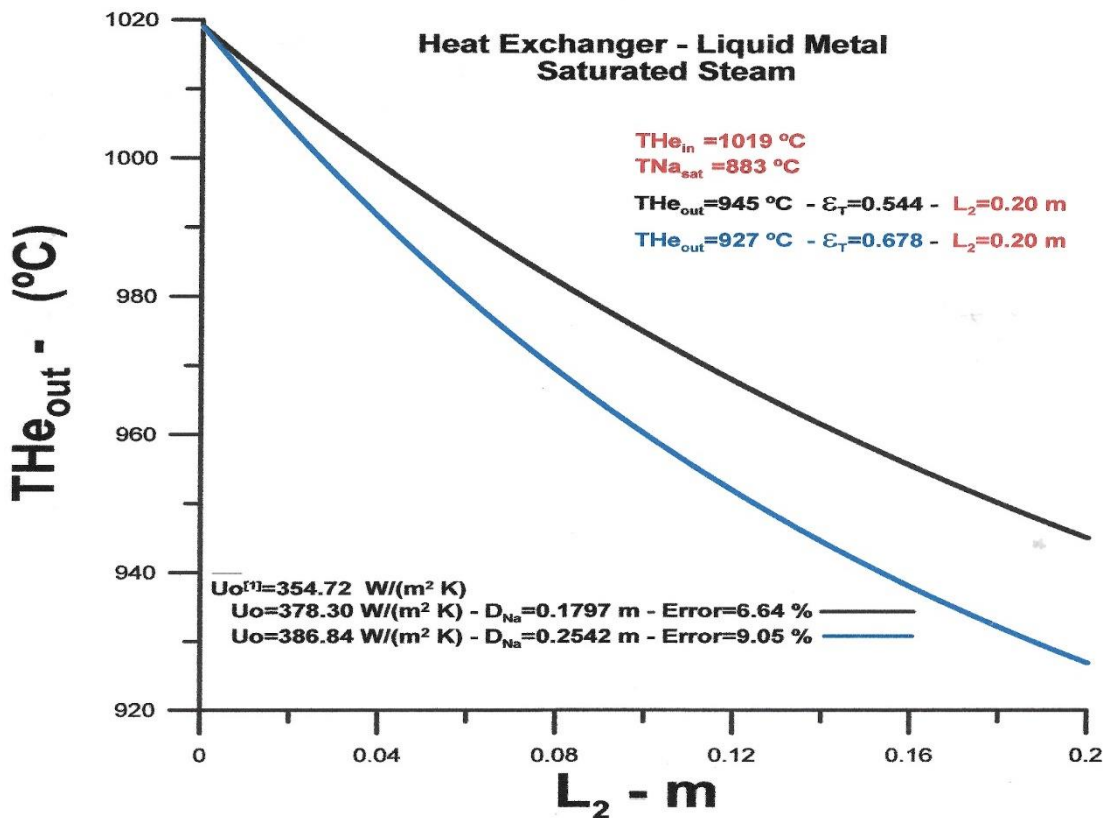


Figure 11 – Outlet temperatures of Helium at the region 2 (Saturated Steam)



SUBCOOLED LIQUID REGION – REGION 3

In region 3, Sodium in the subcooled liquid state enters at a temperature of 120 °C, and Helium enters with a temperature equal to 945 °C when the diameter of the tube associated with Sodium in the saturated vapor region is equal to 0.1797 m, and with a temperature equal to 926 °C for diameter equal to 0.2542.

The absolute deviation obtained for the global heat transfer coefficient in the subcooled liquid region equals 4.43%.

Figure 12 presents results for thermal efficiency in the cooled liquid region, with helium inlet temperatures equal to 945 °C and 926 °C, with values respectively equal to 0.763 and 0.736. The length of the pipe in the cooled liquid region corresponds to 0.80 meters for the first temperature mentioned and 0.86 meters for the second temperature. These results indicate greater heat exchange for the helium inlet temperature equal to 926 °C due to the larger diameter and length of the pipe.

The thermal effectiveness corresponds to 0.884 and 0.864 for the two helium vapor entry conditions, as shown in Figure 13. The highest value obtained for effectiveness corresponds to the largest diameter associated with the saturated vapor region, equal to 0.2542, and an inlet temperature of the helium vapor in the subcooled liquid region equal to 926 °C.

Figure 12 – Thermal efficiency in the region 3 (Subcooling Liquid)

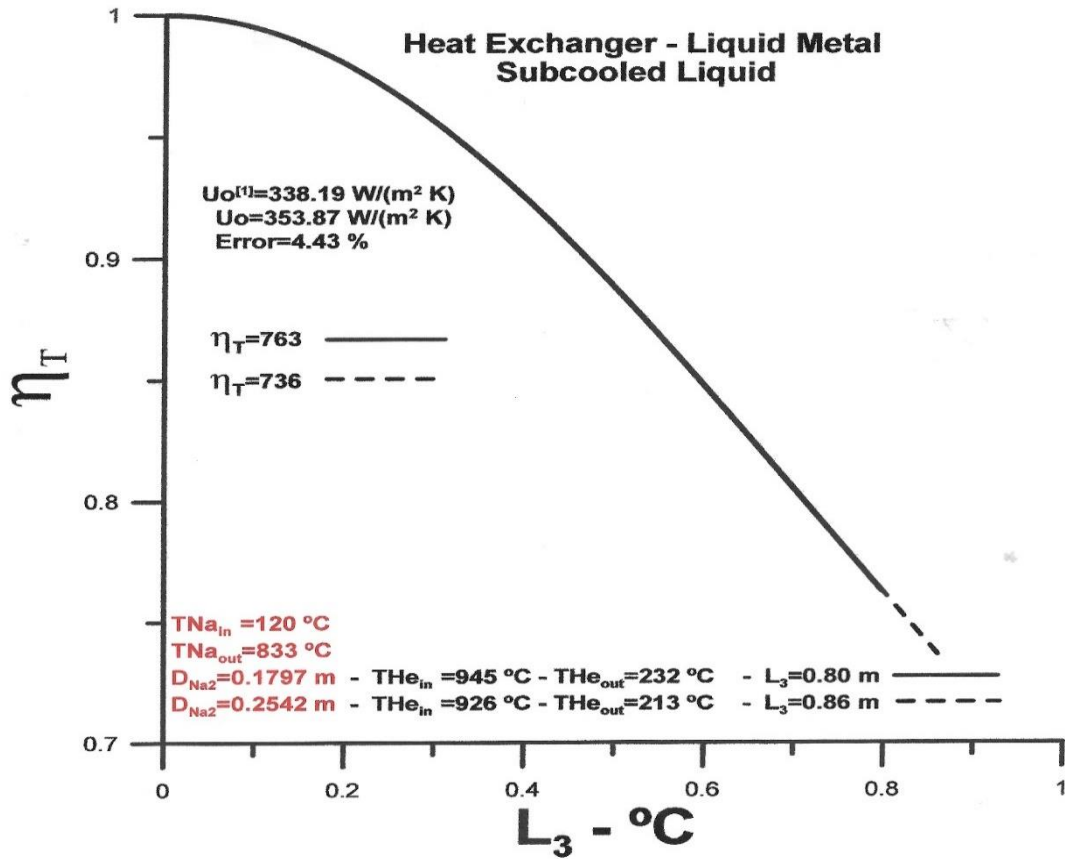


Figure 13 – Thermal effectiveness in the region 3 (Subcooling Liquid)

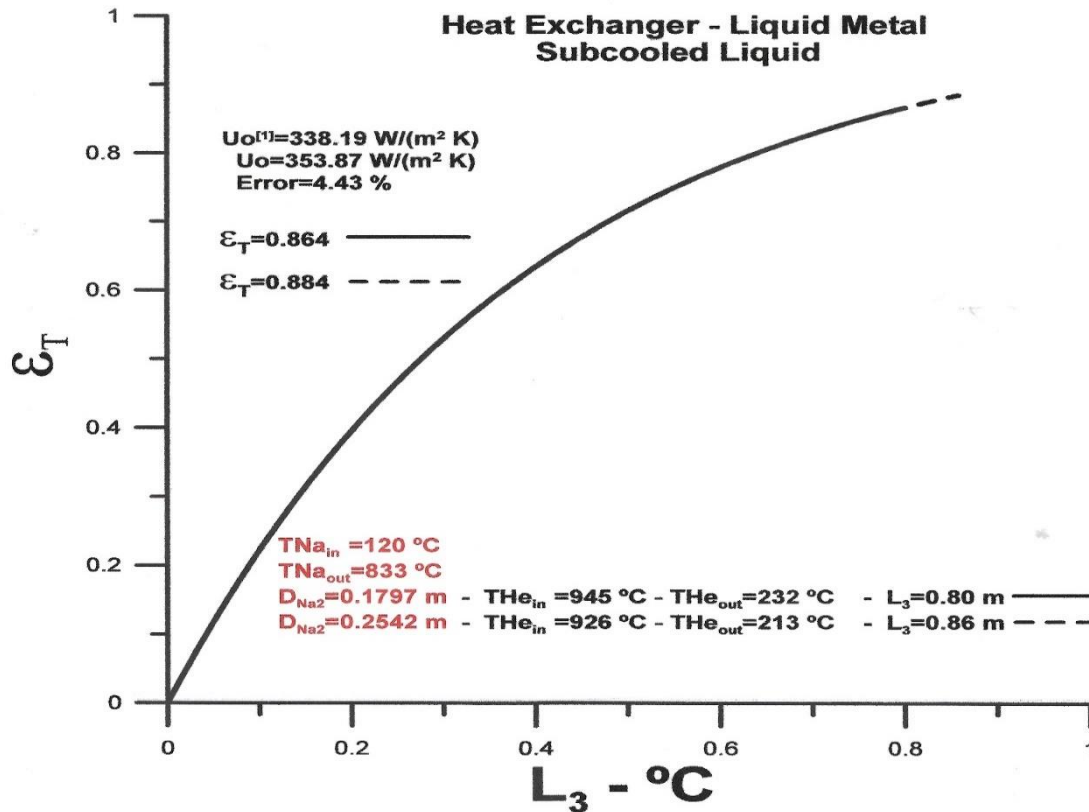


Figure 14 – Heat transfer rate in the region 3 (Subcooling Liquid)

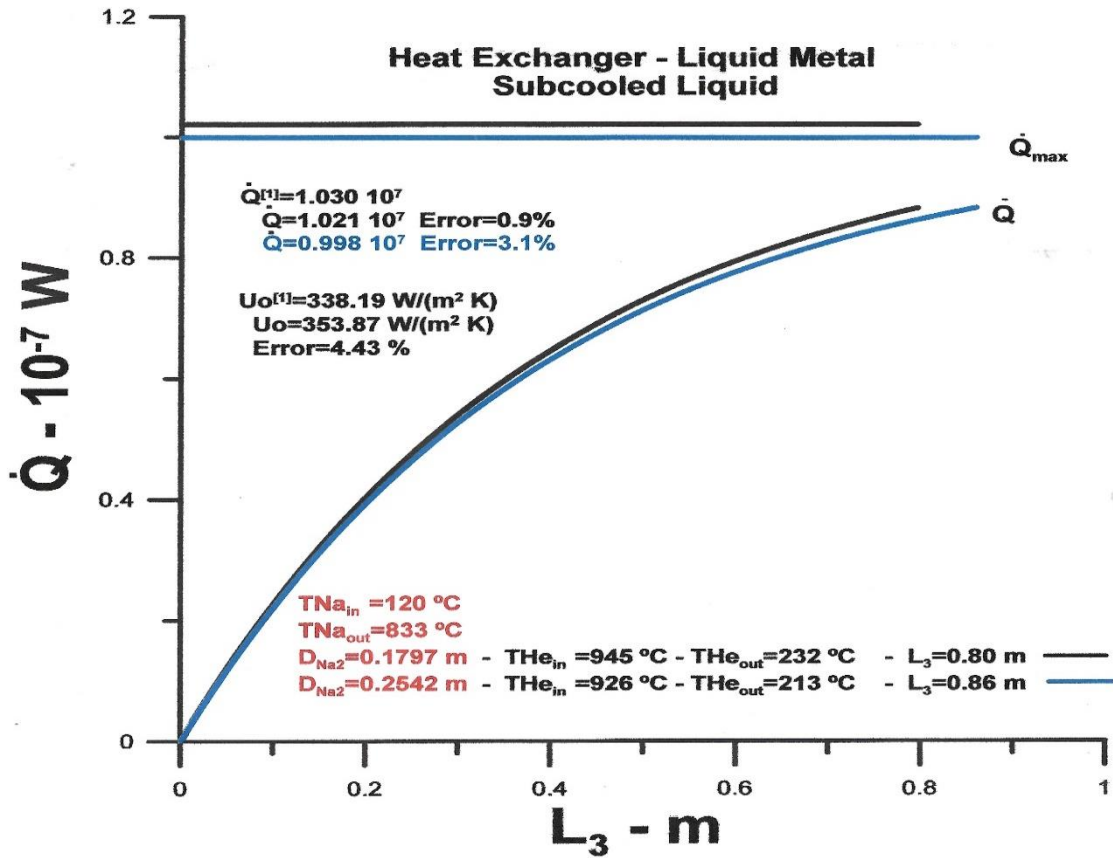
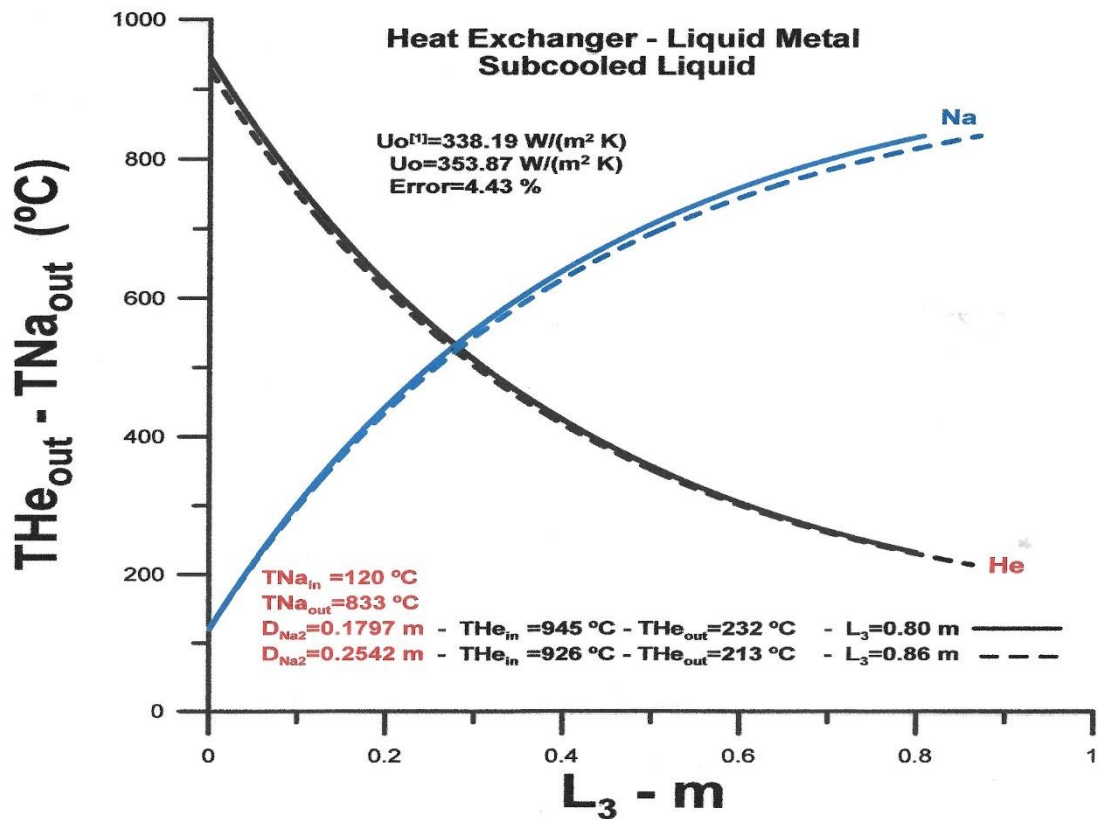


Figure 15 – Outlet temperatures in the region 3 (Subcooling Liquid)



The heat transfer rate in the subcooled liquid region is shown in Figure 14. The absolute deviation determined for the heat transfer rate in region 3, when the helium vapor inlet temperature equals 945 °C, corresponds to 0.9% and is equal to 3.1% when the helium inlet temperature equals 926 °C. Note that the maximum values for heat transfer shown in Figure 14 depend on the difference in inlet temperature between the two fluids that exchange heat and that the sodium inlet temperature value is fixed, equal to 120 °C.

The exit temperatures of the helium and sodium fluids are represented in Figure 15. The sodium exit temperature, equal to 833 °C, determines the other associated quantities. The helium vapor outlet temperatures depend on the stipulated inlet temperatures. The same happens with the length of the pipe. When the sodium inlet temperature is set to 945 °C, the values obtained for the helium outlet temperature and tube length are equal to 232 °C and 0.80 m. When the inlet temperature is 926 °C, the helium outlet temperature is 213 °C, and the section length is 0.86 m.

CONCLUSION

The counterflow Liquid Metal Phase Heat Exchanger was used to simulate the heat exchange process used in a nuclear power plant to produce hydrogen.

The heat exchange process between superheated Helium and liquefied Sodium is carried out in three stages related to Sodium: subcooled liquid stage, saturated steam stage, and superheated steam stage. Helium's inlet temperature equals 1027 °C, and Sodium is 120 °C. The sodium outlet temperature equals 945 °C, and the helium outlet temperature depends on the conditions imposed in regions 2 and 3. The helium outlet temperatures in the simulation correspond to 232 °C and 213 °C.

Comparisons were made with a previously developed model using a different numerical procedure, and the deviations presented did not exceed 13%.

The use of the equation developed by Rhosenow for the nucleated boiling process proved consistent in the simulation presented.

The analytical efficiency method is a powerful tool that makes it possible to analyze situations under different operating conditions, which are not permissible through experimental means due to the high cost involved.

A similar analytical procedure can simulate thermal and viscous irreversibilities using the Bejan number to determine the best configuration for the system in terms of cost-benefit.

NOMENCLATURE

A_{tr} – heat transfer area, [m^2]

C_p – specific heat, [$\frac{J}{kg K}$]



C – thermal capacity, $[\frac{W}{K}]$

C_{\min} – minimum thermal capacity, $[\frac{W}{K}]$

$$C^* = \frac{C_{\min}}{C_{\max}}$$

D_h – hydraulic diameter, $[m]$

Fa – fin analogy number

g – acceleration of gravity

h – coefficient of heat convection, $[\frac{W}{m^2K}]$

He - Helium

k – thermal conductivity, $[\frac{W}{mK}]$

K - Kelvin

L – vertical or horizontal length, $[m]$

\dot{m} – mass flow rate, $[\frac{kg}{s}]$

Na - sodium

Nu – Nusselt number

Pr – Prandtl number

\dot{Q} – actual heat transfer rate, $[W]$

\dot{Q}_{\max} – maximum heat transfer rate, $[W]$

Re – Reynolds number

T – temperatures, $[^{\circ}C]$

U_o – global heat transfer coefficient, $[\frac{W}{m^2K}]$

SUBSCRIPTS

boil – boiling

i – region 1, 2 or 3

in – inlet

out – outlet

sat - saturation



GREEK SYMBOLS

α – thermal diffusivity, [$\frac{m^2}{s}$]

ρ – density of the fluid, [$\frac{kg}{m^3}$]

μ – dynamic viscosity of the fluid, [$\frac{kg}{m s}$]

ν – kinematic viscosity of the cold fluid, [$\frac{m^2}{s}$]

ε_T – thermal effectiveness

η_T – thermal efficiency

ΔT – a difference of temperatures, [$^{\circ}C$]

ACRONYMS

NTU – number of thermal units



REFERENCE

1. Sabharwall, P., Utgikar, V., Tokuhira, A., & Gunnerson, F. (2009). Design of Liquid Metal Phase Change Heat Exchanger for Next-Generation Nuclear Plant Process. *Heat Application, Journal of Nuclear Science and Technology*, 46(6), 534-544. DOI: 10.1080/18811248.2007.9711559
2. Idaho National Laboratory. (2008). Next Generation Nuclear Plant Project Preliminary Project Management Plan. PLN-2489 (INL/EXT-05-00952) Revision 1 [Dennis J. Harrell (2006)]. Retrieved from <http://www.inl.gov>
3. Sabharwall, P., Gunnerson, F., Tokuhira, A., Utgiker, V., Weaver, K., & Sherman, S. (2007). Theoretical Design of a Thermosyphon for Efficient Process Heat Removal From Next Generation Nuclear Plant (NGNP) for Production of Hydrogen. INL/EXT-07-13433. Retrieved from <http://www.inl.gov>
4. Sabharwall, P. (2009). Engineering Design Elements of a Two-Phase Thermosyphon to Transfer NNGP Thermal Energy to a Hydrogen Plant. INL/EXT-09-15383 Revision 0.
5. Shi, S., Liu, Y., Yilgor, I., & Sabharwall, P. (2022). A Two-Phase Three-Field Modeling Framework for Heat Pipe Application in Nuclear Reactors. INL /JOU-21-64836-Revision-0. Retrieved from <http://www.inl.gov>
6. Nogueira, É. (2023). A Theoretical Approach to be Applied in Heat Exchangers by Using the Thermal Efficiency Concept and the Second Law of Thermodynamic. *Mechanical Engineering Advances*, 1(1), 92. <http://dx.doi.org/10.59400/mea.v1i1.92>
7. Nogueira, É. (2023). Localized Theoretical Analysis of Thermal Performance of Individually Finned Heat Pipe Heat Exchanger for Air Conditioning with Freon R404A as Working Fluid. *Journal of Materials Science and Chemical Engineering*, 11, 61-85. <https://doi.org/10.4236/msce.2023.118005>
8. Stojanović, A. D., Belošević, S. V., Crnomarković, N. D., Tomanović, I. D., & Milićević, A. R. (2022). NUCLEATE POOL BOILING HEAT TRANSFER Review of Models and Bubble Dynamics Parameters. *THERMAL SCIENCE*, 26(1A), 157-174. <https://doi.org/10.2298/TSCI200111069S>
9. Taler, D. (2016). Heat Transfer in Turbulent Tube Flow of Liquid Metals. *Procedia Engineering*, 157, 148–157. doi: 10.1016/j.proeng.2016.08.350
10. Ren, L., Tao, X., Zhang, L., Ni, M.-J., Xia, K.-Q., & Xie, Y.-C. (2022). Flow States and Heat Transport in Liquid Metal Convection. *J. Fluid Mech.*, 951, R1. doi:10.1017/jfm.2022.866
11. Petersen, H. (1970). The Properties of Helium: Density, Specific Heats, Viscosity, and Thermal Conductivity at Pressures From 1 To 100 Bar and From Room Temperature to About 1800 K. Risø National Laboratory. Denmark. Forskningscenter Risoe. Risoe-R No. 224.
12. Arp, V. D., & McCarty, R. D. (1989). Thermophysical Properties of Helium-4 From 0.8 to 1500 K With Pressures to 2000 M Pa.
13. Fink, J. K., & Leibowitz, L. (1979). Thermophysical Properties of Sodium. Chemical Engineering Division, Argonne Laboratory, ANL-CEN-RSD-79-1.



14. Golden, G. H., & Tokar, J. V. (1967). Thermophysical Properties of Sodium. Argonne National Laboratory, ANL—7323 Chemistry (TID-4500), AEC Research and Development Report.
15. Kays, W. M., & Crawford, M. E. (1993). Convective Heat and Mass Transfer. McGraw-Hill, Inc., New York.
16. Rohsenow, W. M. (1952). Heat transfer, a Symposium. Engineering Research Institute, University of Michigan, Ann Arbor, Michigan (1952).
17. Chen, J. C. (1963). A Proposed Mechanism and Method of Correlation for Convective Boiling Heat Transfer with Liquid Metals. Brookhaven National Laboratory, BNL 7319 (1963).
18. Fakheri, A. (2007). Heat Exchanger Efficiency. Journal of Heat and Mass Transfer, 129(9), 1268–1276. doi: 10.1115/1.2739620